Gene expression and metabolite changes during *Tuber magnatum* fruiting body storage

Elisa Zampieri2, Flavia Guzzo3, Mauro Commisso3, Antonietta Mello1, Paola Bonfante2 and Raffaella Balestrini1

(1)Istituto per la Protezione Sostenibile delle Piante del CNR, Viale Mattioli 25, 10125 Torino, Italy
(2)Dipartimento di Scienze della Vita e Biologia dei Sistemi, Università di Torino, Viale Mattioli 25, 10125 Torino, Italy
(3)Dipartimento di Biotecnologie, Università di Verona, Strada Le Grazie 15, Ca' Vignal, 37134 Verona, Italy

Abstract
The aim of this study was to investigate the impact of different 4 °C post-harvest storage periods on the quality of the white truffle Tuber magnatum. The expression of selected genes and the profiles of non-volatile metabolites have been analyzed. The up-regulation of genes related to cell wall metabolism and to a putative laccase points to cell wall modifications and browning events during cold storage. Time course RT-qPCR experiments have demonstrated that such transcription events probably depend on the ripening status, since this is delayed in partially ripe fruiting bodies. Changes in the concentrations of linoleate-derived metabolites occur during the first 3 days of considered cold storage, while the other metabolites, such as the amino acids, do not change. Taken together, the results demonstrate that complex molecular events occur in white truffles in the post-harvest period and before they are used as fresh products.

Keywords: Tuber magnatum, Fruiting body, Cell wall, Storage, Quality, RT-qPCR

Introduction
Among the edible fungi, truffles (Tuber spp.) are in particular appreciated in the market because of their organoleptic and flavor properties, both as fresh fruiting bodies and as ingredients in processed products (oil, cheese, pasta, sauce, etc.). Of all the truffle species, the white truffle Tuber magnatum and the black truffle Tuber melanosporum are the most precious, with a request that is much higher than the offer in the food market (Mello et al. 2006). It has already been reported that post-harvest storage can have an impact on mushroom quality (Sakamoto et al. 2009; Eastwood et al. 2011). The aim of the present work was to monitor truffle quality, which is defined as a combination of several parameters (i.e., aroma, flavor, color, size, shape, appearance, and firmness; Hajjar et al. 2010), during post-harvest conservation. Conservation is usually carried out by means of refrigeration (Saltarelli et al. 2008), by irradiation (Nazzaro et al. 2007; Reale et al. 2009) or by modified atmosphere packaging (Rivera et al. 2010), all of which lead to an extension of the shelf life and preservation of the truffle features (i.e., aroma, nutritional value). Some studies have been conducted to monitor the post-harvest quality of truffles. Culleré et al. (2013) and Pennazza et al. (2013) have reported the effect of storage and freezing on the volatile organic compound (VOC) profile, and subsequently on truffle aroma. Saltarelli et al. (2008) have studied the biochemical and microbiological profiles of different truffle species under refrigeration, and have suggested that this procedure is an efficient way of preserving truffle quality. However, little information is available

on the molecular and metabolic events that occur during storage. A low temperature (4 °C) is often utilized to maintain fruiting bodies when they are used as a fresh product, since, according to current gastronomical practices, *T. magnatum* is usually consumed raw. To define some of the events that take place during *T. magnatum* conservation during different 4 °C post-harvest storage periods, both the gene expression of selected genes and metabolite fingerprinting to detect non-volatile metabolites have been verified; new information has been obtained on the processes that occur in the precious fruiting bodies. In particular, attention has been focused, by means of RT-qPCR, on the expression of genes involved in cell wall metabolism, stress tolerance and phenol oxidation considering the results of previous studies on Lentinula edodes and Agaricus bisporus that showed changes in gene expression in the post-harvest period (Sakamoto et al. 2009; Eastwood et al. 2011). Metabolomics has recently been used for quality, nutrition, and food component analysis (Cevallos-Cevallos et al. 2009). In this context, attention has been focused, using HPLC-ESI-MS and HPLC-APCI-MS, on both polar and lipidic metabolite fractions as in a previous study that identified damage markers in A. bisporus post-harvest using a metabolic profiling approach (O'Gorman 2010; O'Gorman et al. 2012).

Materials and methods

Biological materials

Six *T. magnatum* truffle fruiting bodies were selected among those harvested in the same truffle-ground in November 2011 at Montà d'Alba (CN, Italy). The limited number of considered samples was due to the decision to use truffles collected from the same place at the same time, in order to avoid variability due to different geographic locations. These samples were then weighed, cleaned (the peridium was removed) and cut into four pieces. The *T. magnatum* fruiting bodies were divided into two subgroups on the basis of their maturation level, which was measured under a light microscope, counting the number of full asci (Garnero et al. 2000). The first group included three samples, with 30–40 % of full asci that showed a low maturation level; the second group included three samples, with 70–80 % of full asci, showing a high maturation level.

Regardless of the ripening status, the weight of all the samples was about 15 g. A single piece of each truffle was frozen with liquid nitrogen, stored at −80 °C, and was then used as the control (T 0). The other pieces were stored at 4 °C, after having wrapped them in a paper towel and closing them in a glass container, for 3 (T 1), 7 (T 2) and 15 days (T 3) and then stored at −80 °C for the subsequent analyses.

Primer design

T. melanosporum gene models, corresponding to phenol oxidation, cell wall metabolism and heat shock proteins, were used to search the homologs in *T. magnatum* cDNA and DNA through tblastn., primers for RT-qPCR were designed for 21 genes on the basis of the homolog sequence using PerlPrimer, a free, open-source GUI application (http://perlprimer.sourceforge.net/). The primers, listed in Table 1, were tested on the cDNA and DNA of *T. magnatum*. This work was done in the frame of the *T. magnatum* genome sequencing project, therefore the sequences considered in this study were not deposited in GenBank since the *T. magnatum* genome sequence will be published elsewhere (Francis Martin, personal communication).

RNA extraction and cDNA conversion

The RNA was extracted using the Rneasy Plant Mini Kit (Qiagen, Valencia, CA, U.S.A.), according to the manufacturer's instructions. After extraction, the RNA was cleaned of DNA, using Promega DNasi (RQ1 RNase-Free DNase, Promega Corp., Madison, WI, U.S.A.) and measured using a NanoDrop. The absence of genomic DNA was verified through retrotranscription PCR (RT-PCR, OneStep RT-PCR, Qiagen) with the primers for the elongation factor 1a housekeeping gene (Tmaef1a; Table 1). Five hundred ng of total RNA was used to synthesize the cDNA, according to the SuperScript II Reverse Transcriptase (Invitrogen, Life Technologies, Paisley, UK) procedure. The cDNA quality was verified through PCR, using the primer for the Tmaef1a housekeeping gene.

RT-qPCR

Quantitative RT-PCR was carried out with StepOne apparatus (Applied Biosystem–Life Technologies, Monza, Italy). Each PCR reaction was conducted on a total volume of 20 µl, containing 1 µl diluted cDNA (dilution 1:5), 10 µl SYBR Green Reaction Mix and 2 µl of each primer (3 µM), using a 48-well plate. The used primers are listed in Table 1. The following PCR programme, which includes the calculation of a melting curve, was used: 95 °C for 10 min, 40 cycles of 95 °C for 15 s, 60 °C for 1 min, 95 °C for 15 s, 60 for 1 min, and 95 °C for 15 s. All the reactions were performed for three biological and three technical replicates. The baseline range and Ct values were automatically calculated using the StepOne software. In order to compare the data from different PCR runs or cDNA samples, the Ct values of all the genes were normalized to the Ct value of Tmaef1a. The candidate gene expression was normalized to that of Tmaef1a by subtracting the Ct value of Tmaef1a from the Ct value of the candidate gene resulting in ΔCt. Since the slopes of the different samples and replicates in the exponential phase were the same, the expression ratios were calculated, without any PCR efficiency correction, from equation $2-\Delta\Delta CT$ (Livak and Schmittgen 2001), where ΔΔCt represents the ΔCt sample − ΔCt control, and the control is represented by T 0. Statistical analyses were carried out using Rest 2008, version 2.0.7, considering 0.05 as the p value.

HPLC-ESI-MS

Nitrogen frozen pieces of less ripe fruiting bodies, which were collected, treated and stored as described in "Biological materials", were powdered. Two hundred milligrams of powder was resuspended in 10 volumes (w/v) of cold chloroform/methanol (2:1, v/v). The samples were first incubated at −20 °C for 30′, then accurately vortexed for 30″, sonicated at 40 kHz for 15 min in an ultrasonic bath (Falc Instruments, Bergamo, Italy) on ice, and centrifuged at 4,500g for 25′ at 4 °C. The chloroform and methanolic phases were collected and the solvent from each phase was evaporated; the chloroform phase was resuspended with 600 µl of methanol, while the methanol phase was resuspended in 600 µl of methanol/water 90/10 (v/v). The samples were filtered through 0.2 µm pore filters. Three pieces from three different fruiting bodies were used as biological replicates for each time point (T 0, T 1, T 2, T 3), and each sample was analyzed in duplicate. The chloroform phases were diluted with 1/1 (v/v) methanol, while the methanol phases were diluted with 1/1 (v/v) LC-MS grade water (Sigma-Aldrich, St Louis) just before the chromatographic analysis. The polar methanolic fractions were spiked with 0.1 mg/ml of 4-hydroxybenzoic acid as internal standard and analyzed by reverse phase HPLC-ESI-MS (high performance liquid chromatography electro spray ionization mass

spectrometry). The chloroform lipid fractions were spiked with 0.5 mg/ml of palimitic acid as internal standard and analyzed by reverse phase HPLC-APCI-MS (high performance liquid chromatography atmospheric pressure chemical ionization mass spectrometry). Both types of fraction were analyzed in alternate ionization mode, using a Beckman Coulter Gold 127 HPLC system (Beckman Coulter, Fullerton, CA) equipped with a C18 guard column (7.5 × 2.1 mm) and an analytical Alltima RP C18 column (150 × 2.1 mm, particle size 3 μm) (Alltech Associates Inc, Derfield, IL). Two solvents were used: 0.5 % (v/v) formic acid, 5 % (v/v) acetonitrile in water (solvent A), and 100 % acetonitrile (for the methanol phases) or acetonitrile/isopropanol 80/20 (v/v) (for the chloroform phases) (solvent B). For methanolic phases, a solvent gradient was established from 0 to 10 % B in 5 min, from 10 to 20 % B in 10 min, from 20 to 25 % B in 2 min, and from 25 to 70 % B in 7 min. For chloroform phases, a solvent gradient was established from 50 to 80 % B in 2 min, followed by 3 min in 80 % B isocratic phase, from 80 to 100 % B in 5 min, and 35 min in 100 % B isocratic phase. The injection volume was 20 μl per injection. The flow rate was 200 μl/min. The HPLC system was coupled online with a Bruker Esquire 6000 ion trap mass spectrometer, equipped with an electrospray ionization (ESI) source (for the methanolic phase) and an atmospheric pressure chemical ionization (APCI) source (for the chloroform phase). MS data were collected using the Bruker Daltonics Esquire 5.2- Esquire Control 5.2 software, and processed using the Bruker Daltonics Esquire 5.2-Data Analysis 3.2 software (Bruker Daltonik GmbH, Bremen, Germany). The alternate mass spectra were recorded in the 50–3,000 m/z range (full-scan mode, 13,000 m/z/s). MS/MS and MS3 spectra were recorded for the fragmentation pattern analysis of the metabolites in positive and negative mode in the 50–3,000 m/z range, with the fragmentation amplitude set at 1 V. Helium was used as the collision gas. The vacuum pressure was $1.4 \times 10{-}5$ mbar.

For LC-ESI-MS analysis, the other parameters were set as follows: Trap Drive 32.5; Octopole RF Amplitude 152.8 Vpp; Lens 2 −60.0 Volt; Capillary Exit 113.5 Volt; Dry Temp (Set) 350 °C; Nebulizer (Set) 50.00 psi; Dry Gas (Set) 10.00 l/min; HV Capillary 4,500 V; HV End Plate Offset −500 V.

For LC-APCI-MS analysis, the other parameters were set as follows: Trap Drive 46.2; Octopole RF Amplitude 152.8 Vpp; Lens 2 60.0 Volt; Capillary Exit −113.5 V; Dry Temp (Set) 350 °C; APCI Temp (Set) 400 °C; Nebulizer (Set) 50.00 psi; Dry Gas (Set) 5.00 l/min; HV Capillary 2,000 V; HV End Plate Offset −500 V.

Metabolites were identified through a comparison of m/z and the fragmentation pattern with an in-house library of standard compounds and with the data available in the MassBank public database (http://www.massbank.jp/) and in the literature. Chromatogram data extraction and alignment were carried out using MZmine software (http://mzmine.sourceforge.net).

The relative quantitation (i.e., comparison between samples) was based on the area of each of the signals extracted from the chromatograms and expressed as intensity (arbitrary units).

Statistical analysis

Multi Variate Data Analyses were carried out using SIMCA-P+12 software (Umetrix AB, Umea, Sweden). The average value of the two technical replicates of each sample was calculated for each metabolite for these analyses. Principal component analysis (PCA) and orthogonal projection to latent structure discriminant analysis (O2PLS-DA) were performed using the HPLC-ESI-MS putatively identified and quantified

metabolites as the X variables, with scaling based on the Pareto method. The models were cross validated using a permutation test (200 permutations).

Results

Targeted gene expression analysis

In order to verify the molecular changes that occured during truffle conservation, the expression of 21 genes putatively involved in stress tolerance, cell wall degradation/synthesis and phenol oxidation (Table 2; Supplementary Table 1) was analyzed. The stress tolerance genes included putative members of heat shock proteins, such as Tmahsp30_1, Tmahsp90, Tmahspa12a_3, Tmahspa12b, and a putative dehydrin (TmaDHN1). The putative genes involved in the cell wall metabolism, such as chitin synthases (TmachsG and TmachsD), a chitinase (Tmacht2_1), a chitosanase (Tmacho), several glucan 1,3-β-glucosidases (Tmaexg, Tmaexg1, Tmaexg2), a soluble cell wall protein (Tmascw11), a 1,3-β-glucanosyltransferase (Tmagel), a 1,3-β-glucan synthase component FKS1 (Tmafksa), three polysaccharide deacetylases (Tmapda2, Tmapda3, Tmapda5) and a probable glycosidase crf (Tmacrf1) were also considered, in addition to two genes (Tmatyr and Tmalcc) related to tyrosinase and laccase.

The fruiting bodies with 30–40 % of full asci showed an up-regulation at T 2 (after 7 days) for most of the considered genes (Table 2), while the fruiting bodies with 70–80 % of full asci showed a similar up-regulation trend at T 1 (after 3 days) (Table 2). The most up-regulated and the least regulated genes at T 2 were the heat shock protein Tmahspa12a_3 (19.01) and the putative polysaccharide deacetylase Tmapda5 (1.58), respectively, in the less ripe fruiting bodies, and at T 1 the putative glucosidase Tmaexg1 (32.62) and the dehydrin TmaDHN1 (4.46), respectively, in the ripe ones.

Untargeted metabolomics analysis

The LC-ESI-MS and LC-APCI-MS chromatograms of the truffle extracts are shown in Fig. 1. The main metabolites were fragmented and, when possible, putatively identified (Table 3; Supplementary Table 2). The identified polar metabolites included some aminoacids, organic acids and glutathione derivatives.

The fragmentation pattern of most of the less polar metabolites allowed them to be putatively identified as fatty acid derivatives. These molecules, as shown in the example in Fig. 2, showed fragments that were derived from the loss of the carboxyl group and of the oxydryls, which are typical functional groups of hydroxyl fatty acids. Moreover, repetitive loss of 14 atomic mass units, corresponding to the –CH2– group typical of the aliphatic chains, was observed.

Both a decrease and an increase in the level of specific metabolites were observed when the chromatograms of the T 0 and T 3 samples were compared (Fig. 1). In detail, a hydrophobic molecule with m/z 282.5 (Fig. 1, peak 5) disappeared completely during the 4 °C storage, while other polar and hydrophobic molecules increased (Fig. 1, peaks 17, 21, 24, 25 and 26).

The LC-ESI-MS crude analyses were processed using MZmine; in the more polar methanolic phase, 194 signals were detected in negative ionization mode and 140 in positive ionization mode, while in the lipidic chloroform phase, 41 signals were detected in negative ionization mode and 39 in positive ionization mode.

These signals corresponded to metabolites, their isotopes, fragments and adducts.

The untargeted LC-MS metabolite fingerprint approach was selected for data analysis. This sensitive, high throughput and high resolution approach allows to detect differences between samples independently from metabolite annotation. To do this, multivariate analysis techniques were used to handle multiple variables (features) simultaneously and hence also to detect important combinations of features.
The principal component analysis of the two lipid datasets (positive and negative ionization) showed a clear separation between the T 0 and T 3 samples along the first principal component, with the T 1 and T 2 samples showing intermediate behavior (Fig. 3a, b). A great variability between the individual samples, especially within the T 1 and T 2 time points, was also observed (Fig. 3a, b). The principal component analysis of the two polar metabolite datasets (positive and negative ionization) strongly highlighted the individual differences between the three individual fruiting bodies along the first two principal components (Fig. 3c, e), while the third component showed a rough separation according to the sampling time (Fig. 3d, f). Thus, it can be stated that the lipidic components in white truffle are more affected by storage than the polar metabolites, and the storage effect is clear after 15 days. Three days storage did not produce any detectable effect on truffle metabolome.
In order to discover which metabolites were responsible of the observed separation, an O2PLS discriminant analysis was performed using the T 0 samples as class 1 and the T 3 samples (in which a clear effect of storage was observed by means of PCA) as class 2. The O2PLS-DA loading S-plot in Fig. 3, which has obtained by mapping the loading p against the correlation pq(corr), shows the metabolites that were responsible for the separation between the T 0 and T 3 samples in the four dataset (lipids, positive and negative ionization, polar metabolites, positive and negative ionization) (Fig. 4).
Cut-off values for pq(corr) >0.8 and <-0.8 were used to select the metabolites that contributed most to differences between the T 0 and T 3 samples and the others (Supplementary Table 3). Lower cut-offs were used for the T 0-characterizing metabolites of the lipid positive ionization dataset, due to the missing of variable with higher pq(corr) values. Interestingly, beside the decrease in specific metabolites, many metabolites, from all the four datasets, characterized the T 3 rather than the T 0 samples, thus indicating that their level increases during 4 °C storage.

Discussion

It is well known that the features of mushrooms may be affected by post-harvest storage. Since refrigeration is used widely in restoration for the post-harvest storage of white truffles, the effect of several refrigeration times on the expression of selected genes and on the non-volatile metabolite profile of the white truffle *T. magnatum* has been analyzed. The results have shown that gene expression is altered during the storage period. A different regulation has been observed for ripe and less ripe fruiting bodies (T 1 and T 2, respectively), thus suggesting that the considered genes are mostly expressed, under refrigeration, at an advanced maturation level. In addition, metabolomic analysis has shown that the lipidic components are affected more by storage than the polar metabolites, and that the storage effect becomes clear after 15 days (T 3).

The expression of cell wall and stress-related genes is affected by storage

On the basis of previous studies on mushrooms during the post-harvest period (Sakamoto et al. 2009; Eastwood et al. 2011), attention has been focused on the expression of genes involved in cell wall metabolism, stress tolerance and phenol oxidation, by means of RT-qPCR experiments. Considered together, the results have

shown that most of the considered genes were significantly up-regulated ($p < 0.05$) at T 2 (7 days) for less ripe fruiting bodies, and at T 1 (3 days) for the ripe ones, while the same genes were less expressed or not statistically significantly different from T 0 at the other time course points. This regulation (T 1 for ripe and T 2 for less ripe) suggests that the expression of the considered genes is activated under refrigeration, depending on the ripening status, since it is delayed in the less ripe fruiting bodies.

Sakamoto et al. (2009) have demonstrated that genes encoding proteins involved in cell wall metabolism in L. edodes, such as glucanases and chitinases, show an increase in the transcription level 3 days after the harvest. However, the remodeling of the fungal cell wall involves numerous pathways related to both degradation and synthesis. The regulation of *T. magnatum* genes coding for proteins involved in chitin and glucan metabolism has been observed here, suggesting that a cell wall remodeling process occurs, and that texture of fruiting bodies could change during storage. These events are probably also present during the latter ripening stages. Zivanovic et al. (2000) demonstrated that A. bisporus mushrooms simultaneously softened and toughened during post-harvest storage, and showed an increase in chitin content. The herein observed regulation of TmachsG, encoding a putative class III chitin synthase in less ripe fruiting bodies, is in agreement with previous data (Balestrini et al. 2000), which demonstrated that TbCHS3 (a *T. borchii* class III chitin synthase) plays a role during spore cell wall formation, thus suggesting that spore maturation is still in progress. Genes coding for heat shock proteins, which can prevent protein aggregation and assist protein degradation and refolding, also resulted to be regulated during *T. magnatum* post-harvest, unlike what was observed in L. edodes (Sakamoto et al. 2009). Although it is not possible to be sure that the considered genes are homologous in the two fungi, this discrepancy could be due to the great difference in the considered storage temperature, i.e., 25 and 4 °C for Lentinula and Tuber, respectively. It has already been demonstrated that refrigeration (4 °C) has an effect on HSP gene expression in *T. melanosporum* mycelium, and a role of these proteins has been suggested during fungal adaptation to cold (Zampieri et al. 2011). The regulation of TmaDHN1, which shows homology with *T. borchii* TbDHN1 and *T. melanosporum* TmelDHN1, which were previously observed to be differentially expressed during the reproductive stage as well as during the vegetative stage under stress conditions (Abbà et al. 2006; Zampieri et al. 2011), can be explained by the protective role of such a protein during cellular dehydration.

Since tyrosinase and laccase activities have been shown to increase in *L. edodes* after harvest (Kanda et al. 1996; Nagai et al. 2003), *T. magnatum* sequences that code for a putative tyrosinase and laccase, which are involved in monophenols and polyphenols oxidation that can result in melanin synthesis, have been considered. Tyrosinase activity has also been reported in white truffle fruiting bodies, including *T. magnatum* (Miranda et al. 1996). The present results are in agreement with those already reported for L. edodes fruiting bodies (Sakamoto et al. 2009), where a role of these enzymes during browning events has been suggested. The expression for these genes in the white truffle has mostly been observed in less ripe fruiting bodies (at T 2), suggesting that they could be involved in the browning events that occur during maturation, i.e., that lead to changes in the spore cell walls. Phenol oxidases, apart from being involved in lignin degradation, are also involved in diphenol oxidation, melanin production and cell wall building (Zarivi et al. 2013), and a role in cell wall hardening and spore protection has also been suggested for *T. melanosporum* tyrosinase (Zarivi et al. 2011).

Tuber magnatum metabolite fingerprinting

In order to evaluate the effect of cold storage on the metabolite composition of *T. magnatum*, polar and lipidic metabolite fractions were prepared and analyzed through untargeted LC-ESI-MS (for the polar metabolite fraction) and LC-APCI-MS (for the lipid fraction). This approach, which has here been applied to truffles for the first time, allows us to detect both polar and less polar non-volatile metabolites. Moreover, untargeted LC-MS fingerprinting, which is independent from metabolite identification, was used to analyze the datasets, in order to detect the general metabolite modification trend that occurs during cold storage.

With this approach, it has been possible to detect various primary metabolites, some of which were putatively identified, including organic acids, amino acids and fatty acid derivatives. However, phenolic secondary metabolites, such as hydroxybenzoic and hydroxycinnamic acids, which have been described in various black truffle species (Villares et al. 2012), were not detected at all, even though the used analytical approach (metabolite extraction and analysis) was well suitable for the detection of these classes of metabolites. Gallic, gentisic, p-hydroxybenzoic, protocatechuic and p-coumaric acids, have been described in Tuber aestivum, while at least some of them were detected in *Tuber indicum* and *T. melanosporum* (Villares et al. 2012). However, none of these metabolites, whose spectra were included in our in-house library of authentic standard, was detected in *T. magnatum*, possibly indicating that this truffle does not share a similar chemical composition with other Tuber species. The lipidic fraction included mainly derivatives of octadecanoid acids with various degrees of unsaturation and hydroxylation. Fatty acids with 16 and 18 carbons have been described as the most abundant fatty acids in higher fungi (Gao et al. 2001).

The unsupervised PCA showed that, in the fraction containing the more polar metabolites, the differences between individual truffles prevail over the storage induced differences, while the cold storage had more effect on the lipidic fraction of the metabolome. Clear differences were detectable after 15 days of cold storage, while minimal or no differences were evident in samples kept at 4 °C for 3 or 7 days.

Thus, it can be stated that the lipidic portion of the metabolome is more sensitive to cold storage treatment. Among the putatively identified metabolites, one oxidized derivative of linoleic acid (oxylipins) was detected, and this metabolite positively characterized the T 3 samples, indicating that it increased during 4 °C storage. Oxylipins, which comprise a large family of fatty acid-derived molecules, originating from eicosanoic and octadecanoic acids, have been described in many fungi (Brodhun and Feussner 2011). Although a role in life cycle control has been proposed for these compounds, mostly during the sexual and asexual development, knowledge on their physiological functions and biosynthetic pathways in fungi is still scarce (Brodhun and Feussner 2011). Octadecanoid based oxylipins have been found in various Ascomycetes, including Aspergillus species (Mazur et al. 1990, 1991; Jernerén and Oliw 2012), Gaeumannomyces graminis (Brodowsky et al. 1992) and *T. indicum* (Gao et al. 2001). Fungal oxylipins can be involved in regulating morphogenetic and growth processes, in secondary metabolite production as well as in environmental responses. However, knowledge on the effect of these compounds on fungal differentiation is still limited (Brodhun and Feussner 2011). In the *T. magnatum* fruiting bodies studied in this investigation, extensive changes took place in the linoleate-derived metabolites during cold storage, a result that is in line with the induction of genes involved in the fatty acid metabolism observed by Zampieri et al. (2011) in the mycelium of *T. melanosporum* during a cold treatment. In addition, O'Gorman et al. (2012) have indicated pentadecanoic acid, linoleic acid, myo-inositol,

benzoic acid and hexadecanoic acid as the five most important metabolites that could be used as markers for damage in A. bisporus. However, changes observed in the metabolome profile, involved both decrease and increase of specific molecules, while other metabolites, such as aminoacids, did not change during cold storage. This observation is in agreement with data observed by Saltarelli et al. (2008), who have shown that the protein content is not affected in *T. magnatum* at 4 °C, or in another two Tuber species within 15 days.

In conclusion, the results of this study, thanks to both a target gene expression approach and an untarget metabolomic analysis, offer a glimpse of the molecular events that occur during the storage of the precious white truffle fruiting bodies. The gene expression analysis has shown that, under storage, the considered genes are mostly expressed at T 1 and T 2, depending on the fruiting body ripeness, while the metabolic profiles have shown that the T 3 condition is significantly different from that at the starting point and that the lipidic components are affected more by storage compared with the polar metabolites. Attention has so far not been focused on genes involved in lipid metabolism. However, taking advantage of the upcoming *T. magnatum* genome sequence, the several genes involved in lipid metabolism could be identified, and gene expression profiles could be obtained in different conditions, such as during refrigeration. Overall, the presented data represent a first step toward understanding the molecular and metabolic events that take place during fruting body storage.

Acknowledgments

The authors would like to express their thanks to Francis Martin (INRA-Nancy) and his research group for the access to the genome sequences, in the frame of the common Tuber magnatum sequencing project; to Fabiano Sillo and Stefano Ghignone for the support during ESTs analysis, and to Alfredo Vizzini for the morphological evaluation of fruiting bodies ripeness. The research was funded by Regione Piemonte. EZ's fellowship was funded by Regione Piemonte and Turin University.

References

Abbà S, Ghignone S, Bonfante P (2006) A dehydration–inducible gene in the truffle Tuber borchii identifies a novel group of dehydrins. BMC Genomics 7:39

Balestrini R, Mainieri D, Soragni E, Garnero L, Rollino S, Viotti A, Ottonello S, Bonfante P (2000) Differential expression of chitin synthase III and IV mRNAs in ascomata of Tuber borchii Vittad. Fungal Genet Biol 3:219–232

Brodhun F, Feussner I (2011) Oxylipins in fungi. FEBS J 278:1047–1063

Brodowsky ID, Hamberg M, Oliw EH (1992) A linoleic acid (8R)-dioxygenase and hydroperoxide isomerase of the fungus Gaeumannomyces graminis. J Biol Chem 267:14738–14745

Cevallos-Cevallos JM, Reyes-De-Corcuera JI, Etxeberria E, Danyluk MD, Rodrick GE (2009) Metabolomic analysis in food science: a review. Trends Food Sci Technol 20:557–566

Culleré L, Ferreira V, Venturini ME, Marco P, Blanco D (2013) Chemical and sensory effects of the freezing process on the aroma profile of black truffles (Tuber melanosporum). Food Chem 136:518–525

Eastwood DC, Bains NK, Henderson J, Burton KS (2011) Genome organization and transcription response to harvest of two metallothionein-like genes in Agaricus bisporus fruiting bodies. J Microbiol Biotechnol 21:455–463

Gao JM, Wang CJ, Zhang AL, Liu JK (2001) A new trihydroxy fatty acid from the Ascomycete, Chinese truffle Tuber indicum. Lipids 36:1365–1370

Garnero L, Lazzari B, Mainieri D, Viotti A, Bonfante P (2000) TMchs4, a class IV chitin synthase gene from the ectomycorrhizal Tuber magnatum. Mycol Res 6:703–707

Hajjar SE, Massantini R, Botondi R, Kefalas P, Mencarelli F (2010) Influence of high carbon dioxide and low oxygen on the postharvest physiology of fresh truffles. Postharvest Biol Technol 58:36–41

Jernerén F, Oliw EH (2012) The fatty acid 8,11-diol synthase of Aspergillus fumigatus is inhibited by imidazole derivatives and unrelated to PpoB. Lipids 47:707–17

Kanda K, Sato T, Suzuki S, Ishii S, Ejiri S, Enei H (1996) Relationships between tyrosinase activity and gill browning during preservation of Lentinus edodes fruit-bodies. Biosci Biotechnol Biochem 60:479–480

Livak KJ, Schmittgen TD (2001) Analysis of relative gene expression data using real-time quantitative PCR and the 2−ΔΔCT method. Methods 25:402–408

Mazur P, Meyers HV, Nakanishi K, El-Zayat AAE, Champe SP (1990) Structural elucidation of sporogenic fatty acid metabolites from Aspergillus nidulans. Tetrahedron Lett 31:3837–3840

Mazur P, Nakanishi K, Elzayat AAE, Champe SP (1991) Structure and synthesis of sporogenic Psi factors from Aspergillus nidulans. J Chem Soc Chem Commun 20:1486–1487

Mello A, Murat C, Bonfante P (2006) Truffles: much more than a prized and local fungal delicacy. FEMS Microbiol Lett 260:1–8

Miranda M, Zarivi O, Bonfigli A, Porretta R, Aimola P, Pacioni G, Ragnelli AM (1996) White truffles, like black ones, are tyrosinase positive. Plant Sci 120:29–36

Nagai M, Kawata M, Watanabe H, Ogawa M, Saito K, Takesawa T, Kanda K, Sato T (2003) Important role of fungal intracellular laccase for melanin synthesis: purification and characterization of an intracellular laccase from Lentinula edodes fruit bodies. Microbiology 149:2455–2462

Nazzaro F, Fratianni F, Picariello G, Coppola R, Reale A, Di Luccia A (2007) Evaluation of gamma rays influence on some biochemical and microbiological aspects in black truffles. Food Chem 103:344–354

O'Gorman A (2010) Metabolic profiling and fingerprinting for the detection and discrimination of mechanical damage in mushrooms (Agaricus bisporus) during storage. Doctoral Thesis, Dublin Institute of Technology, Dublin, Ireland
O'Gorman A, Barry-Ryan C, Frias JM (2012) Evaluation and identification of markers of damage in mushrooms (Agaricus bisporus) postharvest using a GC/MS metabolic profiling approach. Metabolomics 8:120–132

Pennazza G, Fanali C, Santonico M, Dugo L, Cucchiarini L, Dachà M, D'Amico A, Costa R, Dugo P, Mondello L (2013) Electronic nose and GC-MS analysis of volatile compounds in Tuber magnatum Pico: evaluation of different storage conditions. Food Chem 136:668–674

Reale A, Sorrentino E, Iacumin L, Tremonte P, Manzano M, Maiuro L, Comi G, Coppola R, Succi M (2009) Irradiation treatments to improve the shelf life of fresh black truffles (truffles preservation by gamma-rays). J Food Sci 74:M196–M200

Rivera CS, Blanco D, Salvador ML, Venturini ME (2010) Shelf life extension of fresh Tuber aestivum and Tuber melanosporum truffles by modified atmosphere packaging with microperforated films. J Food Sci 75:225–233

Sakamoto Y, Nakade K, Sato T (2009) Characterization of the post-harvest changes in gene transcription in the gill of the Lentinula edodes fruiting body. Curr Genet 55:409–423

Saltarelli R, Ceccaroli P, Cesari P, Barbieri E, Stocchi V (2008) Effect of storage on biochemical and microbiological parameters of edible truffle species. Food Chem 109:8–16

Villares A, Garcıa-Lafuente A, Guillamon E, Ramos A (2012) Identification and quantification of ergosterol and phenolic compounds occurring in Tuber spp. truffles. J Food Compost Anal 26:177–182

Zampieri E, Balestrini R, Kohler A, Abbà S, Martin F, Bonfante P (2011) The Perigord black truffle responds to cold temperature with an extensive reprogramming of its transcriptional activity. Fungal Genet Biol 48:585–591

Zarivi O, Bonfigli A, Colafarina S, Aimola P, Ragnelli AM, Pacioni G, Miranda M (2011) Tyrosinase expression during black truffle development: from free living mycelium to ripe fruit body. Phytochemistry 72:2317–2324

Zarivi O, Bonfigli A, Colafarina S, Aimola P, Ragnelli AM, Miranda M, Pacioni G (2013) Transcriptional, biochemical and histochemical investigation on laccase expression during Tuber melanosporum Vittad. development. Phytochemistry 87:23–29

Zivanovic S, Buescher RW, Kim KS (2000) Textural changes in mushrooms (Agaricus bisporus) associated with tissue ultrastructure and composition. J Food Sci 65:1404–1408

Table 1 List of primers used in RT-qPCR

Name	Sequence
Tmaef1af	ATTGATGGCTCCTCCAACTG
Tmaef1ar	TTATCGGAAGGACGACTTGG
TmaDHN1f	CGCTACATATACCGGCTCTGCAC
TmaDHN1r	GCCCAAAGTCTTGCTACCATCGAG
Tmahsp30_1f	CCGCCGTGAAGAACCTTAGGA
Tmahsp30_1r	AGCCCTTTCCCGAATCTCCC
Tmahsp90f	GGACTCCCTCTAAATTCACCACC
Tmahsp90r	GGTGTATGAGGAGATGCAGGAG
Tmahspa12a_3f	CATACGGTAGGCAGGTGTAGGG
Tmahspa12a_3r	TAGTTTGTTGAGGGTTCAGGTCGG
Tmahspa12bf	CGGCTCAGTTGCAGTAGACAG
Tmahspa12br	CCGTATCGAAACTACGCATAAGGG
Tmagelf	TCAAGGCACTCATCCGAGAC
Tmagelr	AGTTCAGATAATCTGCCATCTCCC
Tmagpda2f	AAACCCTTTCCCTTCCTCCT
Tmagpda2r	AGGACATTCATTCAGCTCGCT
Tmapda3fnew	CTGGATACCCTCAGCGAGTC
Tmapda3rnew	TTATCACATGGTAGCCCAGG
Tmapda5fnew	GGGTATGGTATCTGTGACGCT
Tmapda5rnew	AATCGTTGAATTCCCCGTAT
Tmacht2_1f	AAGGCTCATCTCCGAGCTCC
Tmacht2_1r	TAGACTGCGCTCCCGATTGAC
Tmagcrf1f	GTTGTCAAGGATGGTAACCTTCTC
Tmagcrf1r	CAACACCCTTGCCATAACTGG
Tmascw11f	TGCTACCTCCTGGAACTCACAC
Tmascw11r	GTAACACCGCCAGCAGTCTC
Tmagchof	GTACTTGTTCCCATCTCTGTAACA
Tmagchor	AGCAACAACATTCCAAGACTTTGA
Tmafksaf	GTGGATGTCATACGGAATCTGGG
Tmafksar	CTGACAACACCCGAATAGGATCTC
TmachsGf	GGCACAATGATGACCATACCCA
TmachsGr	GGTTGTTGCTGGGTGTTAAGGG
TmachsDf	GCGATGATCTCCAGGTTGTCCC
TmachsDr	GCTGCAAATCGCCCTTCGAC
Tmaexgf	GGCTCTCAGAACGGATTCGAC
Tmaexgr	GACTCTGGGCGTAGATTCGG
Tmaexg1f	TCAGACTTGACCTTCAACGGAG
Tmaexg1r	AGTTCCAGTTCATGTAGATCGCAG
Tmagexg2f	AATCGGGTGGTTGAATGGGA
Tmagexg2r	CGTACATAGTCACCACATTCTTGT
Tmagtyrf	TACCGGAACTTTGCATTCTTCTC
Tmagtyrr	TAGACATATGTCCACCGCCAC
Tmaglccf	GGATTCAAGGAATTGCTGGTCA
Tmaglccr	CAACTCTTTCATAACCGTCGAGG

Table 2 RT-qPCR expression values, considering the less ripe (LR) and the ripe (R) *T. magnatum* fruiting bodies at different storage periods ($T_1 = 3$ days; $T_2 = 7$ days; $T_3 = 15$ days)

Gene	Putative function	T_1 LR	T_2 LR	T_3 LR	T_1 R	T_2 R	T_3 R
TmaDHN1	Dehydrin	5.47	7.79	5.43*	4.46	0.75*	1.77*
Tmahspa12a_3	Heat shock protein a12a	10.92	19.01	6.68	18.88	5.24*	4.46
Tmahspa12b	Heat shock protein a12b	4.67	4.41	1.45*	11.47	2.29*	1.10*
Tmahsp30_1	Heat shock protein 30	2.88	2.48	0.81*	5.77	3.24*	0.32*
Tmahsp90	Heat shock protein 90	2.95	6.94	3.36	5.31	2.79*	1.22*
Tmagel	1,3-β-glucanosyltransferase	4.12	6.31	2.60*	19.20	1.20*	1.29*
Tmacht2_1	Chitinase	4.67	4.41	1.45*	3.30*	1.20*	1.49*
Tmascw11	Soluble cell wall protein 11	3.99	4.48	1.73*	16.34	5.06*	3.50*
Tmapda2	Polysaccharide deacetylase	1.82*	2.01*	1.13*	6.06*	3.95*	0.90*
Tmapda3	Polysaccharide deacetylase	1.54*	2.84	0.74*	5.92	0.54*	0.55*
Tmapda5	Polysaccharide deacetylase	1.47*	1.58	0.52*	5.38	0.38*	1.35*
Tmaexg	Glucan 1,3-β-glucosidase	3.23*	5.12	2.29*	5.13	1.02*	1.61*
Tmaexg1	Glucan 1,3-β-glucosidase	3.87	8.26	1.92*	32.62	3.36*	7.18*
Tmaexg2	Glucan 1,3-β-glucosidase	3.86	4.72	2.05*	2.38*	0.40*	0.59*
Tmacho	Chitosanase	5.03	6.77	3.08	2.29*	0.66*	0.95*
TmachsG	Chitin synthase G class-III	7.21	16.54	4.36*	13.35*	4.63*	1.50*
TmachsD	Chitin synthase D class-VI	2.88*	2.43*	0.89*	5.40*	0.41*	0.47*
Tmacrf1	Probable glycosidase crf	7.57	7.87	1.57*	30.84	5.66*	3.15*
Tmafksa	1,3-β-glucan synthase component FKS1	4.03	3.21*	1.62*	12.46*	2.16*	1.62*
Tmalcc	Laccase	2.17*	3.10	0.88*	12.17*	2.05*	2.50*
Tmatyr	Tyrosinase	5.11*	5.08	2.02*	6.78	1.28*	1.40*

* Not statistically significant different ($p > 0.05$) from T_0

Table 3 Characteriation of the main chromatografic peaks of Fig. 1

Peak no.	*m/z* (−)	*m/z* (+)	rt	Putative identification
1		175.2	2.3	Arginine
1		189.2	2.3	*N*-acetyl lysine
2		132.1	3.5	Leucine
3		166.1	5.3	Phenylalanine
4		298.3	7.8	Unidentified
i.s.		139.1	11.9	4-Hydroxybenzoic acid
5		246.3	13	2-Methylbutyroylcarnitine or isovalerylcarnitine
5		263.4	14.4	Unidentified
6	180.8		2.3	Sugar (glucitol)
7	190.7		3.3	Citric acid
8	305		4.6	Unidentified
9	366.1		7.1	Glutathione derivative
10	472.2		9.5	Glutathione derivative
i.s.	136.8		11.6	4-Hydroxybenzoic acid
11	421.2		14.6	Unidentified
12		258.3	2.1	Arginine derivative
13		295.3	9.7	Fatty acid
14		296.3	11	Fatty acid
13		279.5	11.8	Fatty acid
15		282.5	18.4	Fatty acid
16		341.6	22	Unidentified
17		381.5	34.4	Brassicasterol [M-H_2O+H]+
18	387.1		2.5	Di-hexose. fa
18	190.7		2.6	Citric acid
19	327.2		4.2	Unidentified
20	311.2		9.6	9-HPODE
21	476.4		12.8	Fatty acid derivative
22	279.2		18.2	Fatty acid
i.s.	255.7		21.7	Palmitic acid
23	573.7		25	Fatty acid derivative
24	773.1		31.4	MGDG. fa
24	726.6		31.5	MGDG
25	616.9		33.4	C16:0-OH (hydroxypalmitic acid) derivative. fa
25	570.7		34.3	C16:0-OH (hydroxypalmitic acid) derivative
26	600.9		35.2	Unidentified
26	554.4		35.3	Unidentified

The fragmentation trees of these metabolites are reported in Supplementary Table 2

rt retention time, *i.s.* internal standard, *fa* formic adduct

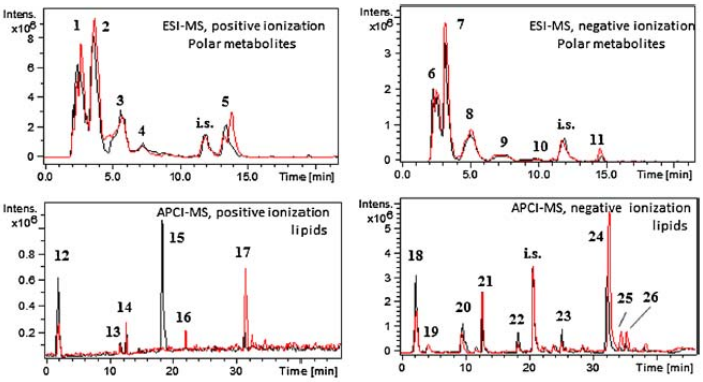

Fig. 1 LC-ESI-MS base peak chromatograms of polar and lipidic fraction of T_0 (*in black*) and T_3 (*in red*) samples, in positive and negative ionization mode

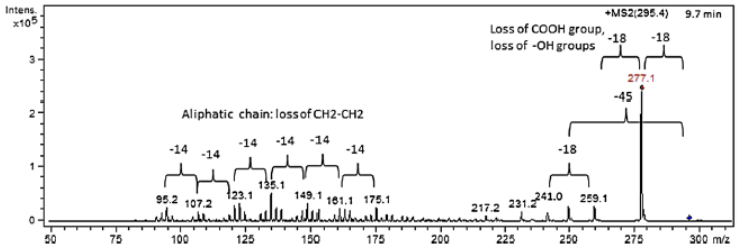

Fig. 2 MS/MS mass spectrum of a putative fatty acid derivatives, with m/z (+) = 295 and retention time (in minutes) of 9.7

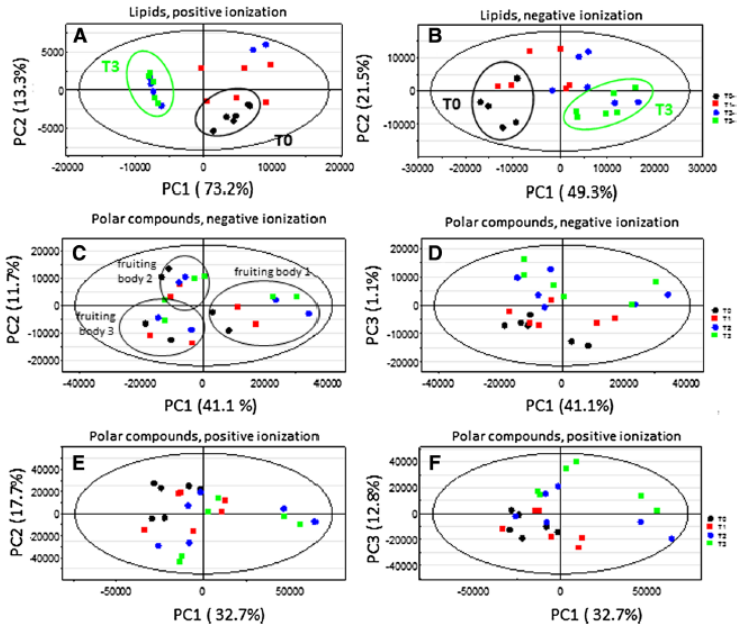

Fig. 3 Multivariate analysis of the four metabolomics datasets. **a**, **b** PCA of the lipid datasets obtained by means of LC-APCI-MS analysis in negative (**c**, **d**) and positive (**e**, **f**) ionization mode. **C**–**F** PCA of the polar metabolite datasets obtained by means of LC-ESI-MS analysis in positive (**a**) and negative (**b**) ionization mode. The *colored dots* of the score scatter plots represent the individual fruiting bodies classified according to the storage time (T_0 = *black*; T_1, 3 days = *red*; T_2, 7 days = *blue*; T_3, 15 days = *green*). Three biological and two technical replicates are shown. The score plots of the PCA models show a clear separation between T_0 (*in black*) and T_3 (*in green*) along the first principal component for lipid datasets, along the third component for polar metabolite datasets. The first and second principal components of PCA of polar metabolite in negative ionization mode datasets clearly separates the individual truffles

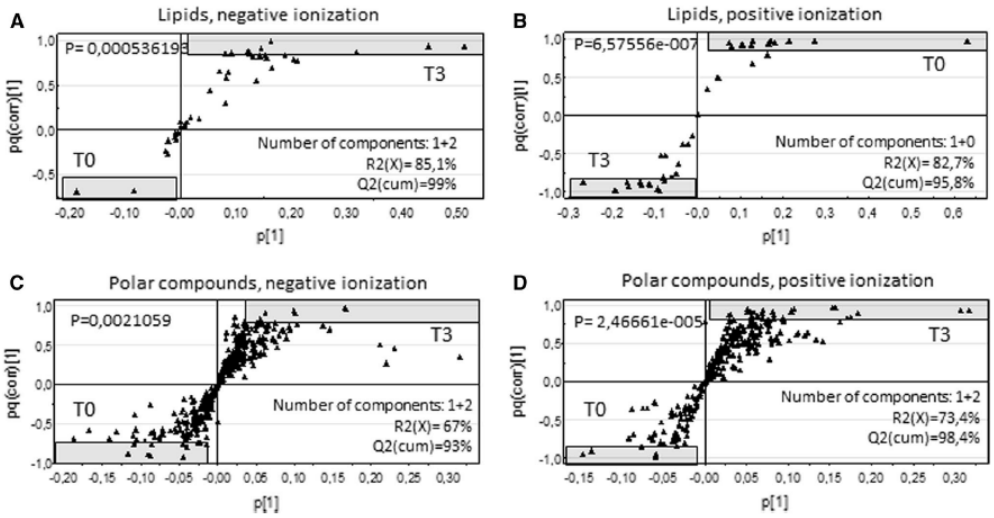

Fig. 4 O2PLS-discriminant analysis of T_0 vesrus T_3 samples: *p* versus pq(corr) loading S-plots of lipid and polar metabolite datasets in negative and positive ionization mode are shown. The metabolites (*black triangles*) that discriminate between T_0 and T_3 are highlighted in *gray*. The models were cross validated through a permutation test (200 permutation) and through ANOVA (the *p* value is reported)